AD_____

Award Number: W81XWH-07-1-0216

TITLE: Development of a Tumor Histologic-Specific, Nano-Encapsulated Contrast for Enhancing Magnetic Resonance Imaging of Prostate Cancer

PRINCIPAL INVESTIGATOR: Joel W. Slaton, M.D.

CONTRACTING ORGANIZATION: University of Minnesota
Minneapolis, MN 55454

REPORT DATE: April 2008

TYPE OF REPORT: Annual

PREPARED FOR: U.S. Army Medical Research and Materiel Command
Fort Detrick, Maryland 21702-5012

REPORT DOCUMENTATION PAGE

Form Approved
OMB No. 0704-0188

1. REPORT DATE	2. REPORT TYPE	3. DATES COVERED
07-04-2008	Annual	5 Mar 2007 - 4 Mar 2008

4. TITLE AND SUBTITLE

Development of a Tumor Histologic-Specific, Nano-Encapsulated Contrast for Enhancing Magnetic Resonance Imaging of Prostate Cancer

5a. CONTRACT NUMBER

5b. GRANT NUMBER
W81XWH-07-1-0216

5c. PROGRAM ELEMENT NUMBER

6. AUTHOR(S)

Joel W. Slaton, M.D., Gretchen Unger, Ph.D., Gregory P, Metzger, Ph.D.

E-Mail: slato001@umn.edu

5d. PROJECT NUMBER

5e. TASK NUMBER

5f. WORK UNIT NUMBER

7. PERFORMING ORGANIZATION NAME(S) AND ADDRESS(ES)

University of Minnesota
Minneapolis, MN 55454

8. PERFORMING ORGANIZATION REPORT NUMBER

9. SPONSORING / MONITORING AGENCY NAME(S) AND ADDRESS(ES)
U.S. Army Medical Research and Materiel Command
Fort Detrick, Maryland 21702-5012

10. SPONSOR/MONITOR'S ACRONYM(S)

11. SPONSOR/MONITOR'S REPORT NUMBER(S)

12. DISTRIBUTION / AVAILABILITY STATEMENT
Approved for Public Release; Distribution Unlimited

13. SUPPLEMENTARY NOTES

14. ABSTRACT
Imaging of both metastatic and localized prostate cancer (CaP) remains a challenge. Our collaborators at GeneSegues, Inc. have developed the nanocapsule, a novel technology that, when coated with antibodies against specific cell types, is capable of delivering large cargos intracellularly into these specific cells. This project proposes to use nanocapsules to carry a contrast agent to human CaP cells growing in mice to enhance MR detection of cancer. Our work in the first year has focused on in vitro construction of a standard nancapsule around a variety of ferrous oxide particle which we have successfully completed. We have demonstrated reproducible in vitro uptake monitored by i) morphology (atomic force microscopy, AFM), ii) surface charge (zeta potential by dynamic light scattering) iii) incorporation (colorometric assay, ICP-AES), iv) cellular proliferation by thymidine incorporation and v) cellular uptake by iron histology. Cue to collapse of 35 W bridge, our MR collaborator's lab was shut down and has now just about to open delaying our in vivo MR work. We have recruited a second MR collaborator, Gregory Metzger, who is assisting with in vitro phantom work.

15. SUBJECT TERMS
Magnetic resonance contrast agents, nanotechnology, prostate cancer

16. SECURITY CLASSIFICATION OF:			17. LIMITATION OF ABSTRACT	18. NUMBER OF PAGES	19a. NAME OF RESPONSIBLE PERSON
a. REPORT	b. ABSTRACT	c. THIS PAGE			USAMRMC
U	U	U	UU	15	19b. TELEPHONE NUMBER *(include area code)*

Standard Form 298 (Rev. 8-98)
Prescribed by ANSI Std. Z39.18

Table of Contents

INTRODUCTION:

Imaging both metastatic and localized prostate cancer (CaP) remains a challenge. Bone scans can identify bone turnover but lack specificity. Literature regarding the value of PET and PET/CT fusion scanning is inconclusive regarding their efficacy. Currently, magnetic resonance imaging using extracellular contrast agent is used primarily to demonstrate extracapsular extension of a bulky localized prostate cancer. The nanocapsule (sub-50 nanometer capsule) is a novel delivery technology, locally produced by GeneSegues, Inc., capable of intracellular delivery of large cargos in a tissue- and cell-specific manner. These nanocapsules derive their specificity from a coating of ligands that have the potential to target tumors of specific histology. This project proposes to use the nanocapsule containing MR detectable contrast agents created magnetic that can be delivered intracellularly to enhance MR imaging of localized and metastatic prostate cancer. Specific Aims: (1) Characterize and compare in vitro uptake of nanocapsules containing agents that can be imaged in vitro (2) Assess in vitro uptake of nanoencapsulated MR contrast agents. (3) Evaluate in vivo uptake and MRI characteristics in human CaP cells growing orthotopically in mice

BODY

A. <u>Nanocapsule Development</u>

In the first year, we proposed to focus on development of a contrast containing nanocapsule that could be targeted to *in vitro* models of prostate cancer. We have elected to focus on tenfibgen coated capsules before proceeding to PSMA antibody containing capsules. The primary contrast agents we have elected to focus on are iron oxide and europium (as a substitute for gadolinium which at high concentrations could be toxic to normal tissue). Europium is a rare earth metal being investigated as a contrast agent for temperature mapping by MRI methods [1]. Europium delivery also enables utilization of a highly sensitive analytical method, neutron activation analysis (NAA) for equivalence with current methods of radiolabel tagging of drug agents and tissue labeling. In NAA, tissue samples containing species tagged with appropriate metals can be made radioactive for traditional gamma counting methods by subjecting samples to irradiation in a nuclear reactor. In **Figure 1**, we performed an initial pilot study executed in prostate tumor-bearing mice using sub-50 nm nanocapsules coated with tenfibgen and bearing, in this case, iodine-derivatized siRNA to allow for assessment of biodistribution of the nanocapsules. Mice were treated with 10 mg/kg of s50 siRNA iodinated at weight percentage of 1% and euthanized 2 hours later. Comparison of tissue iodine levels from mice treated with either drug bearing capsules or empty capsules shows the tenfibgen nanocapsules show excellent accumulation in primary tumors without RES accumulation at 2 hours post-treatment (**Figure 2**). Microscopy of tumors and metastases from NAA mice show that capsules are present in lesions at 2 hours post-treatment connecting the NAA signal to capsule delivery. Europium offers advantages in sensitivity over iodine derivatization in that a larger load of metal can be attributed to each capsule and Europium background is negligible in mammalian tissue.

In our preliminary data, we showed that tumor-specific imaging, supported by histology, could be achieved with a non-homogenous ferrofluid (EMG 805, Ferrofluidics, Nashua, NH) formulated into sub-50 nm tenfibgen nanocapsules. In pilot data, mice were administered a nominal dose of 10 mg/kg and euthanized for imaging 24 hours later. The ferrofluid, while acceptable for proof-of-concept was not intended for use as a biological research reagent. Utilization of this surfactant-stabilized dispersion required significant addition of additional surfactant to mechanical stabilize the dispersion before starting formulation. However, as functional imaging was obtained with this formulation, we designated the s50 EMG-805 formulation as our reference formula.

In our initial formulation studies, we sought to “retarget” or incorporate as a starting material, existing FeO or Eu colloids intended for biological use. We reasoned that colloids prepared for imaging or biological labeling would be more uniform and thus suitable for incorporation into our process. We evaluated prepared colloids (FeO-Eu, Eu) from Biopal (Worcester, MA) and Oceans Nanotech LLC (FeO, Fayetteville, AR). Biopal colloids are used primarily for labeling cells by endocytosis for NAA analysis [2]. We next tested incorporation of nominal 40 nm FeO nanoparticles from Oceans, LLC. Stock concentrations were listed as 10 mg/ml and upon inquiry were found to be determined from microscopy grid measurements creating uncertainty in stock

concentration of iron.

We prepared tenfibgen-coated FeO nanoparticles and compared them to tenfibgen-coated ferrofluid by i) morphology (atomic force microscopy, AFM), ii) surface charge (zeta potential by dynamic light scattering) iii) incorporation (colorometric assay, ICP-AES), iv) cellular proliferation by thymidine incorporation and v) cellular uptake by iron histology. We found that although incorporation is low, nanocapsule targeting is effective enough to provide sufficient cellular accumulation for histology (as well as functional imaging in our preliminary data). Interestingly, zeta potential measurements indicated that s50 nanoencapsulation was able to neutralize surface charge for different starting species morphologies (rod, aggregates) to be tenfibgen-coated (Table 1, -11 vs. –1.4 and –10 vs. +1.2). As s50 oligonucleotide particles, such as the ones used in the Figure 2 biodistribution studies, are also dead neutral, neutral surface charge, together with protein targeting may assist in a larger percentage of particles arriving intact in vivo at target tissue. We have been unable to identify incorporation values from the literature for similar particles to compare our values to, but the improvement in incorporation afforded by moving from a rod-like starting species to 40 nm aggregates (negligible vs. 0.012%) is consistent with pilot formulation studies utilizing hydrophobic small molecules where aggregation of the species into an appropriate size for encapsulation increased drug incorporation (cisplatin vs. condensed cisplatin, negligible vs. 4.1%, unpublished data). Both EMG-805 and Oceans Nanotech NP40 FeO had preexisting surfactant systems that were incompatible with our hydrophobic surfactant system (layer separation was visible in larger batches). However, the efficacy of our reverse micelle process, is supported by the compaction of long rod-like micelles and the breaking up of 40 nm aggregates (Table 1, 'Morphology'). These data indicate that future starting materials require an inherently hydrophobic surfactant system or no surfactant present and point the way towards encapsulation yields approximating our nucleic acid work where we routinely achieve nearly 100% encapsulation. We have recently obtained permission to acquire FDA approved Sinerem, a dextran iron oxide compound, from AMAG Pharmaceuticals, Inc, (Cambridge, MA) to serve as a contrast agent for nanoencapsulation.. This product has been demonstrated to provide negative contrast in cancerous lymph nodes.

Table 1 Characterization Summary for retargeted and naked colloids

Fe Species	Status	Morphology (AFM)	Surface Charge (mev)	Stock Conc. ug/ml (nominal)	Concentration ug/ml (mean, SE)
EMG-805		Long, rod-like	-11 ± 11	500	188 ± 16*
306-18H	Ref. formula	Twisted coils	-1.4 ± 2.7	500	3.0 E-05 ± 4E-06 #
Np40 FeO		40 nm agg.	-10 ± 9.4	50	9.5 ± 0.4**
409-14V	formulated	10-20 nm irreg.	+1.2 ± 1.9	500	1.2 E-02 ± 7E-05#

* ICP-AES with 1 hour of nitric acid digestion at 60°C

** ICP-AES without digestion

Colorimetric assay following acid digestion and dye binding per [3]

For biological characterization, we compared nanocapsules to iron colloids in various cellular assays. These and all other cellular assays were conducted with cells plated on 3-Dimensional scaffolds (Ultramax, Donaldson Co, Mpls, MN) a.k.a. 'nanofibers' coated with 100 pg/ml of model tumor matrix (2:1 Tenascin:Fibronectin, [4]). We and others have shown that plating cells on nanofiber matrices increases membrane caveolae and membrane expression of molecules associated with lipid-raft signaling (unpublished data, [5, 6]). In preliminary uptake studies, we observed no uptake of s50 iron colloids in cells plated on glass and only minimal uptake in cells plated on matrix-coated glass leading to the utilization of coated matrices for further studies. These results are entirely consistent with the nanocapsule's dependence on membrane caveolae for cellular entry and our studies of nanoencapsulated nucleic acids.

We examined the impact of s50 nanoencapsulation on iron colloid biocompatibility using a cell proliferation assay in our test prostate carcinoma cell line where growth is quantitated in the last 18 hours of the 48 hour assay period by incorporation of radioactive thymidine into newly synthesizing DNA to index new cell growth. Using starting volumes 2.5x those used in uptake studies, the ferrofluid used in the reference

formulation showed significant toxicity while the nanoencapsulated species, albeit as a much lower weight loading did not (Table 2). Europium-Dota, another contrast agent of interest for temperature profiling [1], does not show appreciable cellular toxicity with or without nanoencapsulation which is positive for future work. These results are were novel as nanocapsule uptake is mediated by caveolae and trafficks cargo initially to the nucleus. The impact of nuclear delivery of FeO on cell viability at levels that mediate functional contrast was unknown.

Table 2 Cell Survival after 48 hour exposure to contrast agents

Starting Conc.	**EM 805**	**s50 EM 805**	**Eu-Dota** (0.5 mg/ml)	**s50 Eu-Dota**	**Docetaxel** (1 mg/ml)
0.125 ul/ul	15.9 ±15	106.4±5.6	71.6 ±34.5	107 ±25.6	63.8 ± 60
1:2	18.9±15.5	91.5±18.2	113±35.6	95.5±17.4	59 ±12
1:4	38.1±10.8	131.3±47.5	169±74.4	95.2±8	73.1±4
1:8	27.8±15.6	78 ±18.3	128.9±50.2	96.8±30.3	54.1±5.3
1:16	46.0±13	120 ± 34	125.6 ±35	95.7±19.3	82.6±1.5
Volumetric dose for uptake	0.05 ul/ul	0.05 ul/ul			

Cell survival measured by thymidine incorporation into cells plated on protein-coated 3D scaffolds in 96 well plates. Contrast data is the average of 4 duplicate repetitions.

We evaluated nanocapsule and iron colloid cellular uptake in cells plated in 3D culture using DAB-enhanced Prussian blue histology with Fast Red as a predominantly nuclear counterstain (Perl's Prussian blue, [7]). Iron uptake is reflected by an orange to red shift in color. Nanofiber scaffolds consist of a 300-500 um fibrillar structure highly reminiscent of collagen, mounted on an optically clear plastic substrate with cells populating throughout scaffold. For histology, cultures were developed in 12 well plates, flipped and mounted on glass slides and viewed through the plastic supporting substrate as a 'coverslip'. As the culture is not a monolayer, cells could be best imaged which were closest to surface of plastic substrate (or the bottom of the culture). Figure 3 illustrates a pulse-chase of single dosing on cellular uptake over time. Cultures were treated with equivalent volumes from suspensions with different starting FeO concentrations due to incomplete incorporation (s50, 586 pg, 1.5 pg (np vs. ferrofluid), naked, 0.5 ug, 9.5 ug (np vs. ferrofluid)). Interestingly, uptake in the iron nanoparticle pair appears to peak between 12 and 18 hours (3A3, 3B3). This suggests that cells are able to process iron delivered by nanocapsules. In contrast, cellular uptake in vitro appears to be peaking at greater than 18 hours (3C5, 3D5). The simplest explanation for these in vitro differences is that s50 nanoparticles are 'heavier' and sink to interact with cells more effectively than s50 ferrofluid. In our nucleic acid work, we routinely spike bismuth (MW 207) into capsule crystallization baths to make particles heavier for improved in vitro results. However, these differences may need further investigation.

The most striking observation, however, is that cellular uptake is still comparable between formulated and unformulated species despite 1000x differences in culture loading, highlighting the efficiency of s50 tenfibgen targeting (Fig. 3: A3 vs. B3, C5 vs. D5). This suggests that nanocapsule targeting enables an approximate 1000x improvement cell accumulation (Fig. 3 A3@586 pg vs B3F@0.5 ug). These results support continued development of s50 nanocapsules for MRI contrast.

B. MRI Imaging Development

We had proposed to move our in vivo work into magnetic resonance imaging stage by month 9-12 of year one. Unfortunately as a result of the collapse of the 35W bridge in August of 2007 in Minneapolis, the laboratory of our MR collaborator, Bruce Hammer, Phd,which was nearby, was closed. (http://minnesota.publicradio.org/display/web/2007/10/31/mribridge/s There has been a long delay in identifying a new location for his lab equipment. It now appears that his lab will reopen at the beginning of July of 2008

In the meantime, we have identified an additional collaborator, Gregory Metzger, PhD, who is a member of the Center for Magnetic Resonance Research (CMRR) at the University of Minnesota (see attached

biosketch). The CMRR has 9 different magnets ranging from 1.5 to 9 tesla with a 16 tesla magnet being built. We have begun working with Dr. Metger to develop phantoms to model imaging based on 12 well plate for 3-dimensional cultures used in in vitro studies. tumor (see **Figure** 4).

In our future work, we will pursue two strategies to further improve incorporation of iron into tenfibgen nanocapsules; i) continue with retargeting existing FeO colloids using Investigational Combidex (ferumoxtran-10, Amag Pharmaceuticals) or oleic acid-capped nanoparticles prepared in choloroform (Oceans Nanotech) as starting materials and ii) combine our nanoencapsulation strategy with well-established procedures for precipitating maghemite to synthesize starting materials not burdened by potentially competitive surfactant systems [8, 9]. We will also begin assessing the ability to coat iron particles with PSMA antibody. Simultaneously, we will begin in vivo MR work assessing the reproducibility MR imaging of nanoencapsulated agents we have already produced.

KEY RESEARCH ACCOMPLISHMENTS:

- Developed two nanoencapsulated contrast agents one containing iron oxide and one containing europium
- Demonstrated the ability to visualize in vivo uptake of nanocapsules
- These agents have reproducible uptake into prostate cells in vitro
- Reproducible phantom for assessing in vitro iron content by magnetic resonance imaging

REPORTABLE OUTCOMES:

Development of two nanoencapsulated contrast agents one containing iron oxide and one containing europium

Production of a reproducible phantom for assessing in vitro content by magnetic resonance imaging.

CONCLUSION:

In our first year we have completed production of two nanoencapsulated one containing iron oxide and one containing europium for in vivo monitoring. These agents have reproducible uptake into prostate cancer cells in vivo. WE have also developed a magnetic resonance phantom for assessing in vitro iron content in prostate cancer cells. In year 2 will begin in vivo work using MR to monitor uptake as well as determine if PSMA can be used to coat nanocapsules.

REFERENCES for Body:

1. Li, A., et al., *A sensitive PARACEST contrast agent for temperature MRI: Eu3+-DOTAM-glycine (Gly)-phenylalanine (Phe).* Magn Reson Med., 2008. **59**(2): p. 374-81.
2. Freyman, T., et al., *A quantitative, randomized study evaluating three methods of mesenchymal stem cell delivery following myocardial infarction.* Eur Heart J., 2006. **27**(9): p. 1114-22.
3. Petri-Fink, A., et al., *Development of functionalized superparamagnetic iron oxide nanoparticles for interaction with human cancer cells.* Biomaterials, 2005. **26**(15): p. 2685-94.
4. Huang, W., et al., *Interference of tenascin-C with syndecan-4 binding to fibronectin blocks cell adhesion and stimulates tumor cell proliferation.* Cancer Res., 2001. **61**(23): p. 8586-94.
5. Nur-E-Kamal, A., et al., *Three dimensional nanofibrillar surfaces induce activation of Rac.* Biochem Biophys Res Commun., 2005. **331**(2): p. 428-34.

6. Schindler, M., et al., *A synthetic nanofibrillar matrix promotes in vivo-like organization and morphogenesis for cells in culture.* Biomaterials, 2005. **26**(28): p. 5624-31.
7. Arbab, A., et al., *Characterization of biophysical and metabolic properties of cells labeled with superparamagnetic iron oxide nanoparticles and transfection agent for cellular MR imaging.* Radiology, 2003. **229**(3): p. 838-46.
8. Bee, A., R. Massart, and S. Neveu, *Synthesis of very fine maghemite particles.* J Magn. Mag. Mater., 1995. **149**: p. 6-9.
9. Thünemann AF, S.D., Kaufner L, Pison U, Möhwald H, *Maghemite nanoparticles protectively coated with poly(ethylene imine) and poly(ethylene oxide)-block-poly(glutamic acid).* Langmuir, 2006. **28**(22): p. 2351-7.

APPENDICES

BIOGRAPHICAL SKETCH

NAME Metzger, Gregory	POSITION TITLE Associate Professor
eRA COMMONS USER NAME gmetzger	

EDUCATION/TRAINING *(Begin with baccalaureate or other initial professional education, such as nursing, and include postdoctoral training.)*

INSTITUTION AND LOCATION	DEGREE *(if applicable)*	YEAR(s)	FIELD OF STUDY
University of Pennsylvania, Philadelphia, PA	B.S	1988 - 1992	Bioengineering
University of Minnesota, Minneapolis, MN	Ph.D.	1994 - 1997	Biomedical Engineering

PROFESSIONAL EXPERIENCE
1994 - 1997 University of Minnesota, Minneapolis, MN: (Radiology) Research Assistant
1997 - 2002 Philips Medical Systems, Dallas, TX: Clinical Scientist
2003 - 2005 Philips Medical Systems, Bethesda, MD: (National Institutes of Health) Senior Clinical Scientist
2005 - present University of Minnesota, Minneapolis, MN: (Radiology) Associate Professor

HONORS
1998 Radiological Society of North America: Certificiate of Merit: Scientific exhibit presentation

MEMBERSHIPS
1996 - present International Society for Magnetic Resonance in Mediciine
2006 - present Cancer Center, University of Minnesota

PUBLICATIONS
* Metzger GJ, Patel M, Hu X: Application of Genetic Algorithms to Spectral Quantification. J Magn Reson Series B 1996; 110:316-320.
* Metzger GJ, Hu X: Application of Interlaced Fourier Transform to Echo-planar Spectroscopic Imaging. J Magn Reson Series B 1997; 126:166-170
* Metzger G, Sarkar S, Zhang X, Heberlein K, Patel M, Hu X: A Hybrid Technique for Spectroscopic Imaging with Reduced Truncation Artifact. Magn Res Imag 1999; 17(3):435-443
* Sarkar S, Heberlein K, Metzger GJ, Zhang X, Hu X: Applications of High-resolution Echoplanar Spectroscopic Imaging for Structural Imaging. J Magn Reson Imaging 1999; 10(1):1-7
* Metzger GJ, Szczepaniak LS, Nurenberg P, Mollevanger L: Respiratory Triggered 1H Renal Spectroscopy In Vivo with Short Echo Time. Proc Inter Soc for Magn Reson in Med Seventh Scientific Meeting and Exhibition, Denver, Colorado, (2000)
* Metzger GJ, Szczepaniak L, Sagalowsky AI, Ewalt DH, Nurenberg P: Proc Inter Soc for Magn Reson in Med Ninth Scientific Meeting and Exhibition, Glasgow, Scotland, (2001)
* Weatherall PT, Evans FG, Metzger GJ, Saborrian MH, Leitch AM: MRI vs. Histologic

Measurement of Breast Cancer following Chemotherapy: Comparison with X-ray Mammography and Palpation. J Magn Reson Imaging 2001; 13(6):868-875
* Rappard G, Metzger GJ, Fleckenstein JL, Babcock E, Weatherall P, Adams C, Miller S, Purdy PL: SSFP MR Guided Catheter Navigation of the Intracranial Subarachnoid Space. Am J Neuroradiol 2003; 24:626-629
* Szczepaniak LS, Dobbins RL, Metzger GJ, Sartoni-D'Ambrosia G, Arbique D, Vongpatanasin W, Unger R, Victor RG: Fatty Heart: Myocardial Steatosis and Systolic Function in Humans. Magn Reson Imaging 2003; 49:417-423
* Metzger G, Krieger A, Guion P, Ferhanoglu O, Choyke P, Menard C, Ataler E: Predicting True SAR Limits for In Vivo Imaging in MR Guided Prostate Procedures. Proc 5th Intl Interventional MRI Symposium, #703, Boston, MA, (2004)
* Metzger, G.J., Snyder, C., Can, A., Vaughan, T., Ugurbil, K., Local B1+ shimming for prostate imaging with transceiver arrays at 7T based on subject-dependent trnamit phase measurements, Magn. Res. Med., 59(2): 396-409, 2008
* Ocak I, Bernardo M, Metzger G, Barrett T, Pinto P, Albert PS, Choyke PL. Dynamic contrast-enhanced MRI of prostate cancer at 3 T: a study of pharmacokinetic parameters. AJR Am J Roentgenol 2007;189(4):849.
* Rappard G, Metzger GJ, Weatherall PT, Purdy PD: Interventional MR Imaging with an Endospinal Imaging Coil: Preliminary Results with Anatomic Imaging of the Canine and Cadaver Spinal Cord. Am J Neuroradiol 2004; 24:835-839
* Singh AK, Krieger A, Lattouf JB, Guion P, Grubb RL, Albert PS, Metzger G, Ullman K, Smith S, Fichtinger G, Ocak I, Choyke P, Menard C, Coleman J. Patient selection determines the prostate cancer yield of dynamic contrast-enhanced magnetic resonance imaging-guided transrectal biopsies in a closed 3-Tesla scanner. BJU Int 2007.
* Metzger G, Bernardo M, Thomasson D, Gharib A, Choyke P: Parallel Imaging with a Combined Endorectal-Surface Coil at 3T in Dynamic Contrast Enhanced MRI Studies of the Prostate. Proc Intl Soc Magn Reson in Med 11, #490, Miami, (2005)
* Metzger G, Kozerke S, Murdoch J, El-Sharkawy AM, Bernardo M: 3DSI Prostate Spectroscopy at 3T: Comparison of Multi-Element Coil Combinations. Proc Intl Soc Magn Reson in Med 11, #1946, Miami, (2005)
* Metzger G, Thomasson D, Bernardo M, Choyke P: Towards the Absolute Quantitation of DCE-MRI Pharmacokinetic Parameters: Addressing the Assumption of Constant Contrast Reagent Relaxivity and its Effect on Ktrans. Proc Intl Soc Magn Reson in Med 2006: 14: #386
* G. J. Metzger, I. Ocak, M. Bernardo, and P. Choyke, Quantification of prostate spectra at 3T using LCModel with a simulated basis set, Proc. Intl. Soc. Magn. Reson. in Med. 15, #802, Seattle WA, 2007
* G. J. Metzger, M. Marjanska, and P-G. Henry, Prostate spectroscopy analysis with LCModel: development of 3T scoring criteria,Proc. Intl. Soc. Magn. Reson. in Med. 15, #3668, Seattle WA, 2007
* G. J. Metzger, P-F. Van de Moortele, C. J. Snyder, J. T. Vaughan1, and K. Ugurbil, Local B1 shimming for imaging the prostate at 7 tesla, Proc. Intl. Soc. Magn. Reson. in Med. 15, #799, Seattle WA, 2007.

UNIVERSITY OF MINNESOTA

Twin Cities Campus ***Center for Magnetic Resonance Research*** *2021 Sixth Street SE*
Medical School *Minneapolis, MN 55455*
Tel: (612) 626-2001
Fax: (612) 626-2004

Joel Slaton, MD
Associate Professor
Department of Urologic Surgery
University of Minnesota
Staff Urologist
VAMC, Minneapolis
Email: slato001@umn.edu
Phone: 612-467-3460

April 15, 2008

re: letter of support

Dear Joel

It would be my pleasure to serve as a co-investigator on your CDMRP grant, development of a histology-specific nanoencapsulated contrast agent for enhancing magnetic resonance imaging of prostate cancer. As you know at the Center for Magnetic Resonance Research, we have magnets ranging from 3.0 to 9.4 Tesla for in vitro and in vivo imaging. I will work with you to establish in vitro phantoms for assessing contrast uptake as well as imaging both formalin preserved and live tumor bearing mice that have been injected with the contrast agents.

I look for to working with you on this fascinating project.

Sincerely,

Greg Metzger, Ph.D.
Associate Professor
Department of Radiology
Center for Magnetic Resonance Research.
2021 6th Street SE
Minneapolis, MN 55455
gmetzger@cmrr.umn.edu

FACILITIES

Center for Magnetic Resonance Research (CMRR)

CMRR: The studies will be conducted at the Center for Magnetic Resonance Research (CMRR) which has a research laboratory located in a 30,000-sq. ft. building on the main campus. The CMRR is an NIH funded BioTechnology Regional Resource (BTRR) and is equipped with one of the first 4.0 Tesla human whole-body MRI scanners, a 7.0 Tesla human whole-body MRI Scanner and a 9.4 Tesla 65cm whole-body MRI Scanner. The CMRR also houses a 4.7 Tesla/40cm animal NMR system and a 9.4 Tesla/31 cm horizontal animal NMR system and a 3 Tesla/90 cm Siemens Trio Clinical MR instrument (whole body human system). All scanners are dedicated to basic and clinical research.

CMRR: Clinical Research Center:

Human studies are administered by the General Clinical Research Center (GCRC) Rms. 111F, 111A, 111D, 111G, 111 and 115A within the CMRR are dedicated to Clinical Research.

CMRR: Animal

A 4788 sq. ft. animal facility is present in the same building that houses CMRR. This is a fully equipped facility managed by the University of Minnesota Research Animal Resources.

CMRR: Office

CMRR: At the CMRR, there is Administrative support space (~ 400 sq. ft), for the 4 member support staff at the CMRR. All offices are located in the CMRR.

Other:

CMRR: Machine shops/Electronics shop: Machine shops are available at the Physics Department and at the CMRR. A full electronics shop (~500 sq.ft.) is located within the CMRR and is used for building RF probes, and developing physiological monitoring and recording systems for use in the MR scanner. Additional space in the existing CMRR facility that support the overall biomedical research effort include 1) a conference room/library (~1300 sq. ft), 2) storage (250 sq. ft), 3) Wet Lab space (~1000 sq. ft).

Multi-channel Digital Receivers

All of the human systems have multi-channel digital receivers allowing for parallel imaging techniques that require simultaneous sampling of MR signals from independent probes. The current capabilities of the different systems are:

- 3T: 8 channels (provided with the standard Siemens console)
- 4T: 4 channels (upgrade for 24 channels under progress)
- 7T: 32 channels
- 9.4T/65cm bore: 16 channels

For the 4T, the 7T and the 9.4T/65cm bore, each of the multiple receiver channels consists of individual RF mixers to generate an IF at 20 MHz which are oversampled at 64MHz by 14 bit ADCs on Echotek digital receiver boards (Echotek, Huntsville AL). The digital receiver boards are housed in a VME64x card cage chassis.

Computer

Each of the MR instruments at the CMRR has a console host computer. The scanners with Varian consoles (4.7T, 9.4T 31cm, 4T and 9.4T 65cm) use Sun Blade or Ultra model workstations while the Siemens 3T & 7T scanners uses Windows-XP PCs. Each of the 16 channel digital receiver systems also has its own Sun Blade model workstations as a host computer to handle the streams of multi-channel data. There are 4 compute nodes with dual core 3.8GHz processors used for processing k-space data. For post-processing image space data there are 4 compute nodes, three dual core nodes with 3.6GHz processors and one 8 core node (4 CPUs of Opteron 875 Dual-Core 2.2GHz) with 16GB Ram for parallel processing.

In total for all data processing, physiologic monitoring, paradigm presentation and manuscript preparation, the CMRR is equipped with 23 Sun workstations, 40 Linux servers, and 195 desktop computers (143 Windows, 34 Mac, and 18 Linux). These computers are organized into research groups, with a Sun or Linux computer as the group server. The group servers typically have a 1 to 3 Ghz processor with 2GB of RAM and are used to

handle an aggregate of over 22TB of RAID storage. There are two 22-slot LTO Tape libraries that can backup over 13TB per set of media.

In addition, the CMRR hosts a node of the NIH Biomedical Informatics Research Network (BIRN), a nationwide network of Internet-2 connected computer systems. The BIRN node includes 1TB of RAID storage and four Linux hosts to support distributed high-performance computing and data sharing between institutions at gigabit speeds.

SUPPORTING DATA:

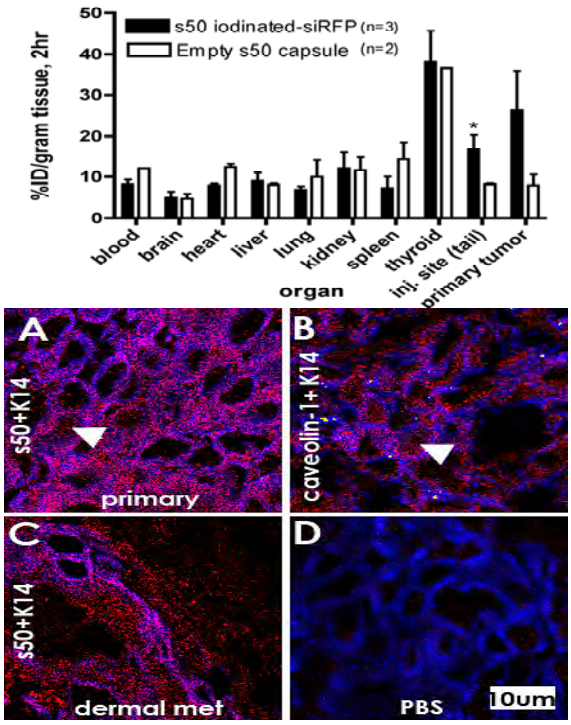

Fig. 1. s50 tenfibgen siRNA-bearing capsule biodistribution is tumor-specific, and homes to metastastic as well as primary tumor. Graph: Biodistribution mice bearing PC-3 xenograft tumors were measured at 2 hours via nuclear activation analysis (NAA) of iodine-128 derivatized siRNA encapsulated in s50 tenfibgen capsules (black bars). Natural levels of tissue iodine were measured in tumor-bearing mice treated with empty tenfibgen capsules (open bars). Tumor and injection site are primary sites of s50 tenfibgen siRNA-bearing capsule accumulation at 2 hours postinjection timepoint (black minus open bars). While non-tumorbearing lymph nodes are difficult to find for comparative purposes, capsules also accumulated significantly in enlarged lymph nodes in the metastatic PC-3 model. No accumulation occurred in the organs of the RES. Micrograph: Cryosections from NAA mice were double-labeled with anti-K-14 (Covance, 'blue Cy5', A-D) to label tumor cells and either goat anti-Syrian Hamster (Jackson, 'red' Cy3 A,C,D) to label capsules or anti-Caveolin-1 (Santa Cruz, 'blue Cy5', B) to label lipid rafts and examined on a Nikon Clsi confocal microscope at x600**.** s50 capsules could be readily detected in primary tumor (A, red) and dermal metastases (C, red), but not untreated K-14(+) tumor (D) thus relating increased I-128 signal to capsule delivery. The pattern of immunosignal for s50 capsules and caveolin-1 was similar in primary tumor supporting lipid raft uptake for s50 capsules in vivo as well as in vitro (arrows, A vs. B).

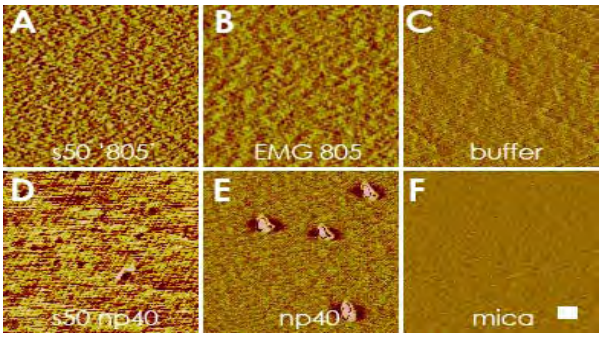

Fig. 2. AFM of "retargeted" FeO colloids. Suspensions were prepared for AFM by dilution to a nominal 1 ng/ml in buffer (18 ohm water for B, PBS + 10% lactitol for others) and 'spotting' onto tape-stripped mica (3M#600) and dried in air. Particles were imaged in tapping mode using a 125 Fm long silica cantilever type IBMSC (IBM) using a Nanoscope II multimode AFM (Digital Instruments) with a J type scanner and ambient tapping mode holder. Bar equals 50 nm.

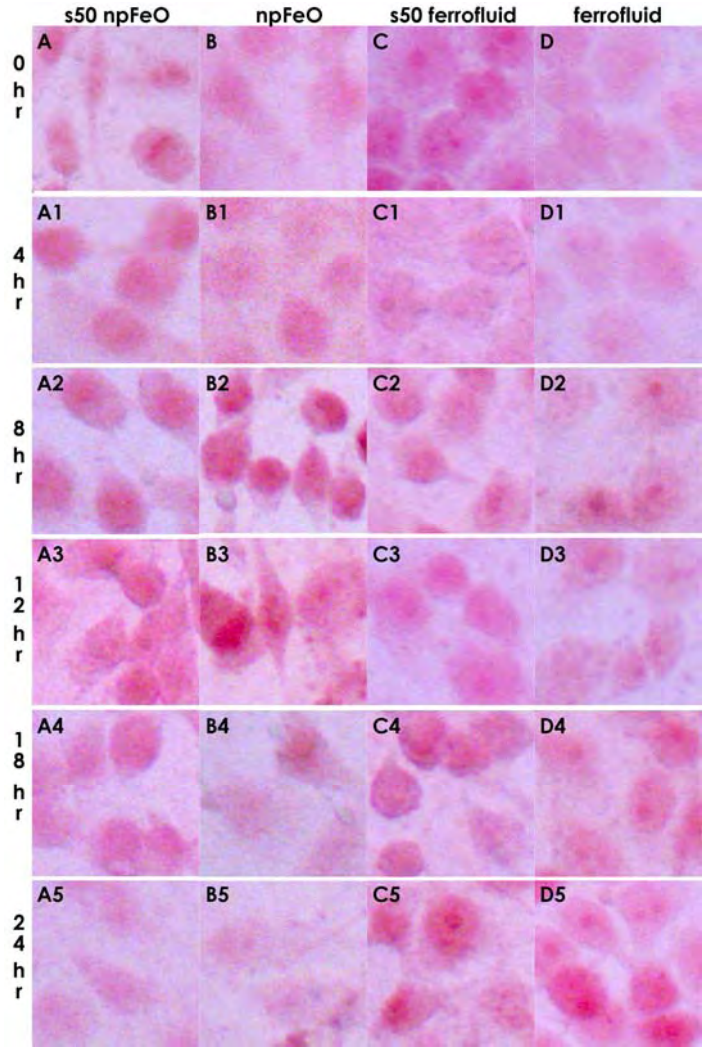

Fig. 3 Timecourse of nanocapsule and iron colloid uptake in prostate carcinoma cultures. Matrix-coated, 3-D nanofiber scaffolds were seeded with 500,000 PC3 prostate carcinoma cells in 0.01% FCS media and treated with 50 ul in 1 ml of media of (A) 2.3 ng Fe by s50 FeO nanoparticles, (B) 1.9 ug Fe by naked FeO nanoparticles, (C) 1.5 pg Fe by s50 ferrofluid, or (D) 9.5 ug Fe by naked ferrofluid. Treatment of cultures was staggered so that exposure times varied from 4 hours over 8, 12, 18 and 24 hours as labeled. Cultures were fixed in 2% paraformaldehyde, developed with DAB-enhanced Prussian blue for iron and counterstained with Fast red. Cultures were mounted on glass sides and imaged using a Canon Sureshot via a Zeiss Axiostar microscope at an approximate power of 240. Experiment is representative of 2-3 repetitions.

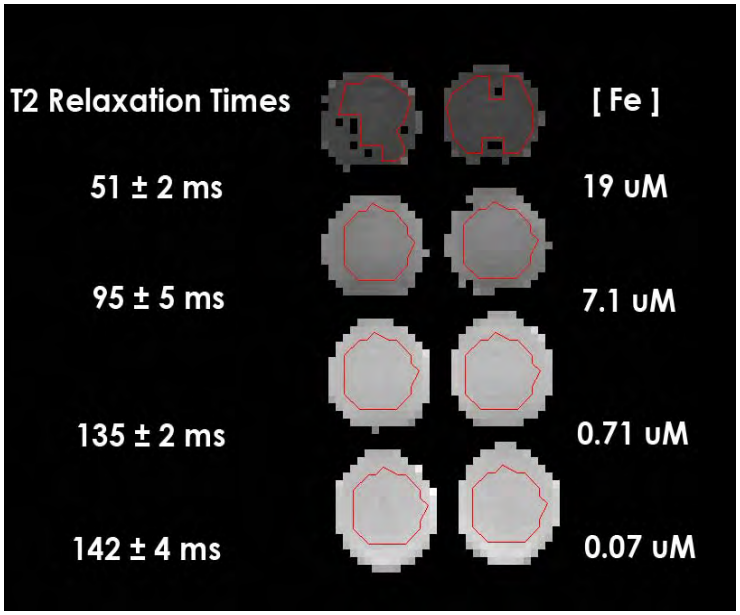

Figure 4. Development of MRI phantom suitable for 3-D cultures. Iron nanoparticles were dispersed in 1200 ul of agarose and capped with an additional 400 u of agarose in 12 well plates. Iron concentrations in dilution stocks were determined by ICP-AES. The phantom was imaged with a multi-echo spin echo acquisition with a 3mm slice thickness and a 1 mm in-plane resolution allowing 32 profiles to be acquired for the calculation the transverse relaxation time (T2). The acquired profiles occurred at echo times of 13 ms to 419 ms in steps of 13 ms. The T2 map was calculated by fitting a line to the natural log based signal intensity versus echo time on a pixel-wise basis. The results show excellent sensitivity through the micromolar range of iron particles